Soret coefficient of isotopic Lennard-Jones mixtures and the Ar-Kr system as determined by equilibrium molecular-dynamics calculations

R. Vogelsang and C. Hoheisel
Theoretische Chemie, Ruhr-Universität Bochum, Universitätsstrasse 150, D-4630 Bochum, Federal Republic of Germany

G. V. Paolini and G. Ciccotti
Dipartimento di Fisica, Università degli Studi di Roma, "La Sapienza," Piazzale Aldo Moro 2, I-00185 Roma, Italy
(Received 17 December 1986)

The Soret coefficient (thermal diffusion coefficient) characterizing the coupling between heat and mass transport in more-component systems has been obtained by equilibrium molecular dynamics. Two-component liquid systems of the Lennard-Jones type were considered: three isotopic mixtures and Ar-Kr. Computations 20 times longer than the ones used for a "usual" transport coefficient, as the thermal conductivity, were necessary to obtain this cross coefficient with modest accuracy. The analysis of the Green-Kubo integrand shows that, opposite to the thermal conductivity, the thermal diffusion depends strongly on the terms containing the partial enthalpies of the components. For the isotopic mixtures, it was found that the Soret coefficient grows with the mass ratio in a way consistent with experimental results. For the Ar-Kr system, direct comparisons with nonequilibrium molecular-dynamics data indicated good agreement. As experimental Soret coefficients for Ar-Kr are lacking, we cannot compare our results with data of the real mixture. The order of magnitude found agrees, however, with that experimentally observed for binary liquid mixtures.

I. INTRODUCTION

While in a pure liquid the collective mass current is zero, in a binary mixture, mass and heat currents couple giving rise to cross transport coefficients, the *thermal diffusion coefficients*, D_α^T, where α $(=1,2)$ refers to the component of the mixture.

These coefficients must not be confused with the *thermal diffusivity*, D_T, being the thermal conductivity, λ, divided by the mass density and the heat capacity of the system. Experimentally, one determines the so-called *Soret coefficients* s_α, being essentially the ratio of these cross coefficients and the mutual diffusion coefficient D_{12}:

$$s_\alpha = -D_\alpha^T/(D_{12}T\rho w_1 w_2) \quad \text{with } \alpha = 1 \text{ or } 2 \ ,$$

where T denotes the temperature, ρ the mass density, and w_1, w_2 the mass fractions.[1]

The effect of diffusion induced by a temperature gradient in binary liquid mixtures was first observed by Ludwig and later by Soret. Thus it is usually termed as the Ludwig-Soret effect.[2] The inverse effect is known as the Dufour effect. Due to Onsager's relations these two cross coefficients are equal.[3] Sometimes cited in the literature are the *thermal diffusion ratios*, $k_{T\alpha}$, which represent dimensionless quantities defined by the ratio of D^T and D_{12}:

$$k_{T\alpha} = D_\alpha^T/(D_{12}\rho w_1 w_2) \quad \text{with } \alpha = 1 \text{ or } 2 \ .$$

These ratios are zero for a pure liquid and nearly zero for highly diluted binary mixtures.[4]

For a binary mixture the Soret coefficients and all the related quantities of the two components must be equal but for a sign. We have, for example,

$$s_1 = -s_2 \ .$$

The subscript is therefore omitted in the following, and s, D^T, and k_T denote the quantities of the *first component.*

For real two-component liquids, the thermal diffusion ratio is at least 1 order of magnitude smaller than 1. Thus the Soret coefficient amounts to about 10^{-3} K^{-1}.[2] We shall confirm this order of magnitude for our model mixtures.

We present here molecular dynamics (MD) calculations for the thermal diffusion coefficient of ideal mixtures in which the particles of the two components differ only in mass. This choice of the mixtures has some advantages which are discussed in later sections.

The Green-Kubo integral is used for the determination, and the analysis of the correlation functions is given in terms of the partial functions. A discussion of the accuracy of the results is furthermore presented using independent runs with varying system size of the MD ensemble.

Furthermore, extensive results for the Ar-Kr model mixture are given and compared with values obtained by using nonequilibrium MD.[5,6] The coefficients for the mutual diffusion and the thermal conductivity are additionally compared, as they are byproducts of the calculations for the cross coefficients.

II. MUTUAL DIFFUSION, THERMAL CONDUCTIVITY, AND THERMAL DIFFUSION FOR A BINARY MIXTURE IN TERMS OF THE GREEN-KUBO RELATIONS

The mutual diffusion coefficient D_{12} can be defined as the time integral of the autocorrelation function of the mass current of the particles of component 1 of the mixture

$$D_{12}=\frac{Q}{3N}\frac{1}{m_1 m_2 w_1 w_2}\int_0^\infty \langle \mathbf{J}_m(0)\mathbf{J}_m(\tau)\rangle d\tau \ , \tag{1}$$

where

$$\mathbf{J}_m(\tau)=m_1\sum_{i=1}^{N_1}\mathbf{v}_i(\tau) \ . \tag{1a}$$

m_1 and m_2 denote the masses of the two species. w_1 and w_2 denote the mass fractions, N the particle number, Q a thermodynamic factor, and $\mathbf{v}_i$ the velocity of a particle i. The total number of particles is given by $N=N_1+N_2$, and the parentheses indicate the thermal average.

This expression is discussed at length in Refs. 7 and 8, and results for the D_{12} are presented in Ref. 9. In what follows, we omit the factor Q giving the D_{12} values for thermodynamically ideal mixtures.

Following Gubbins,[10] we have the Green-Kubo expressions for the thermal conductivity λ, and the cross coefficient (thermal diffusion coefficient) D^T, in the form

$$\lambda=\frac{1}{3Vk_BT^2}\int_0^\infty \langle \mathbf{J}_q(0)\mathbf{J}_q(\tau)\rangle d\tau \ , \tag{2}$$

where $\mathbf{J}_q$ is the heat current given by

$$\mathbf{J}_q=\sum_{\alpha=1}^{2}\sum_{j=1}^{N_\alpha}\tfrac{1}{2}m_\alpha \mathbf{v}_{j\alpha}^2\mathbf{v}_{j\alpha}-\tfrac{1}{2}\sum_{\alpha=1}^{2}\sum_{\beta=1}^{2}\sum_{j\neq k}^{N_\alpha N_\beta}\left[\mathbf{r}_{j\alpha k\beta}\frac{\partial\phi(r_{j\alpha k\beta})}{\partial \mathbf{r}_{j\alpha k\beta}}-\phi(r_{j\alpha k\beta})\underline{\mathbf{e}}\right]\cdot\mathbf{v}_{j\alpha}-\sum_{\alpha=1}^{2}h_\alpha\sum_{j=1}^{N_\alpha}\mathbf{v}_{j\alpha} \ , \tag{2a}$$

$$D^T=\frac{1}{3Vk_BT}\int_0^\infty \langle \mathbf{J}_m(0)\mathbf{J}_q(\tau)\rangle d\tau \ . \tag{3}$$

The subscripts α,β count the two different kinds of particles and j,k count the numbers of particles of a given kind. The term in large parentheses on the right-hand side of (2a) is a dyadic and $\underline{\mathbf{e}}$ is the unit tensor. $\phi(r)$ denotes the interaction potential depending only on the absolute value of the distance vector $\mathbf{r}_{j\alpha k\beta}$, and k_B denotes the Boltzmann constant. h_α is the average enthalpy per molecule of species α. Note that D^T divided by the total mass density and the mass fractions has the same dimensions as D_{12}, length^2/time.[10,11]

Equation (2a) requires some comment. To define the heat current in a two-component system, it is reasonable to substract from the energy current that part of the current associated with macroscopically observable transport of energy. What remains is the part associated with the microscopic motion of the molecules. Thus we have the additional term in Eq. (2a) which involves the partial enthalpies of the components.[11–14] These partial enthalpies h_α, are pure thermodynamic quantities[15] and cannot be defined in terms of simple molecular expressions. Evaluation of these quantities by computer calculations requires additional methods of determination,[16] of which one is presented in Sec. VII.

However, in some special cases, for example, for an isotopic mixture the partial enthalpies may exactly be described by molecular terms, the potential energy and the virial sum of particles of species α relative to those of the same species and of species β, and the kinetic energy of particles of type α. In that case it is also possible to express these thermal averages in instantaneous molecular variables, as shown by MacGowan and Evans.[5]

In this work we have determined h_α by thermal averages over molecular quantities during the MD computation of the heat and mass currents. We have moreover shown by pilot runs that the Evans formulation leads to identical results. For not very nonideal mixtures, the molecular approximation for h_α and thus the Evans formulation of the heat current might be valid (see Sec. VII).

III. MIXTURE SYSTEMS, POTENTIALS, STATES

We have chosen isotopic model mixtures for our investigation to have an exact molecular description of the

TABLE I. Lennard-Jones potential parameters for the considered mixture systems.

	σ_{11} (Å)	σ_{22} (Å)	σ_{12} (Å)	$\epsilon_{11}k_B^{-1}$ (K)	$\epsilon_{22}k_B^{-1}$ (K)	$\epsilon_{12}k_B^{-1}$ (K)	Comment
Systems 1–3[a]	3.519	3.519	3.519	141.445	141.445	141.445	
Ar-Kr[b]	3.405	3.670	3.5375	119.8	167.0	141.445	Lorentz-Berthelot combining rules

[a]System 1, mass ratio, $m_1/m_2=0.7143$ (atomic mass of component 1, 51.56 a.u.). System 2, mass ratio, $m_1/m_2=0.5$ (atomic mass of component 1, 41.25 a.u.). System 3, mass ratio, $m_1/m_2=0.4$ (atomic mass of component 1, 35.36 a.u.).
[b]Atomic mass of argon, 39.95 a.u.; atomic mass of Kr, 83.8 a.u.

TABLE II. Thermodynamic states: $n^* = (N/V)\sigma_x^3$; $T^* = Tk_B/\epsilon_x$; $z = PV/Nk_BT$ (compressibility factor); N, number of particles; V, volume; x_i, mole fraction; σ_x and ϵ_x are defined according to the one-fluid approximation. For systems 1–3, $\sigma_x = 3.519$ Å; $\epsilon_x k_B^{-1} = 141.445$ K. For Ar-Kr, $\sigma_x = 3.540$ Å; $\epsilon_x k_B^{-1} = 143.75$ K.

State point	n^*	T^*	z	x_1	Comment
1	0.7500	0.96	0.35	0.5	For systems 1–3
2	0.8031	0.81	0.2	0.5	Ar-Kr
3	0.7902	0.80	−0.1	0.5	Ar-Kr

partial enthalpies of the components and to study the mass dependence of the Soret effect in the simplest way. Three mass ratios were used and the Lennard-Jones (LJ) potential interaction was employed. Numerical values for the potential parameters are listed in Table I together with the mass ratios. A thermodynamic state has been considered which gave a positive pressure of about 100 bar. Detailed values are presented in Table II.

Furthermore, to compare with nonequilibrium molecular-dynamics (NEMD) and to predict a value for a measurable system, we studied the LJ mixture Ar-Kr at similar state points investigated by NEMD. Lennard-Jones interaction parameters and masses for the Ar-Kr mixture are summarized in Table I. The state point data can be found in Table II. The slight enhancement of the σ_{Kr} LJ potential parameter compared with the usually employed one leads to a positive pressure for state 2 and is thus better suited to model the experimental system.[17]

IV. COMMENTS ON THE COMPUTATIONS

In previous investigations of LJ mixtures, we have found that the mutual diffusion coefficient and thermal conduction coefficient are accessible by MD calculations with an accuracy of about 5% using 5×10^4–10×10^4 integration steps and small particle numbers.[8,9,18] The amplitude of the autocorrelation function (ACF) of the diffusion and the heat currents are sufficiently large, and the time behavior allows a quickly converging integration.[19]

The determination of the Soret coefficients requires, however, the evaluation of a cross-correlation function (CCF) which usually is of much smaller amplitude than either of the ACF's. This has already been shown in Ref. 20. In the case of thermal diffusion, we found for the CCF an amplitude of order 10% of those of the associated ACF's in agreement with findings obtained by NEMD studies.[5,6] For this CCF to achieve an accuracy equivalent to that of the ACF's, the statistical error must be reduced to about $\frac{1}{10}$ of that for the ACF's. Hence, the number of integration steps ought to be enlarged by about a factor of 100. As we are only able to perform about 1×10^6 time steps, a much larger statistical error for the cross transport coefficient is expected. In view of this, we have not attempted to study the particle number and the potential cutoff dependence of the results. Runs of about 10^6 steps, with a cutoff of $(2.25$–$2.5)\sigma$ and a particle number of 108–256, have been performed. Usable technical details of these computations are summarized in Table III. Highest accuracy for the cross coefficient was achieved for system 2 and the Ar-Kr system at state 2. For each of these mixtures, 6–7 independent runs of considerable total time length were carried out. The CCF of system 2 may be compared with the ACF's of the mass and the heat current in Fig. 1.

TABLE III. Technical details of the equilibrium MD.

Particle numbers	108–256 (standard 108)
Integration time steps	10^5–10^6 (standard 8×10^5)
Time step	10^{-14}–2×10^{-14} s (standard 2×10^{-14} s)
Cutoff radii for the Lennard-Jones potentials	2.25–$2.5\sigma_{ij}$
CPU time for 100 integration steps (Cyber 205) in seconds	0.965(108); 2.95(256)

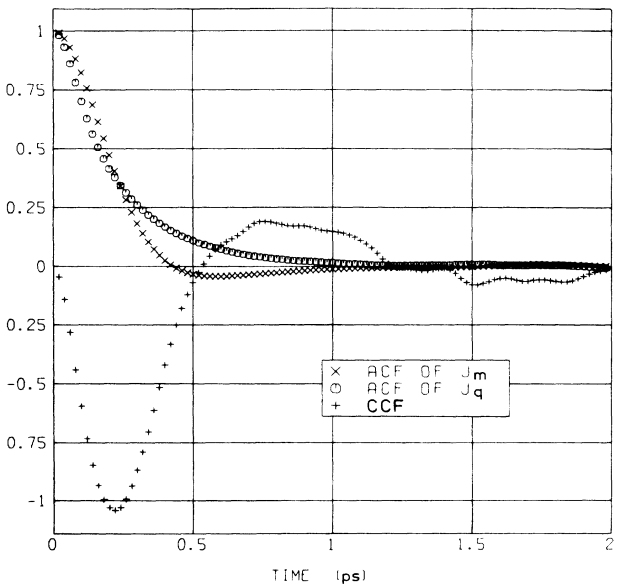

FIG. 1. Green-Kubo integrands for the mutual diffusion, the thermal conductivity, and the thermal diffusion coefficients. The autocorrelation functions are normalized to unity. The cross-correlation function (CCF) is given in units of 10^{10} cm^2/s^2. Integration of the CCF gives $(3/\rho)D^T$ (see Sec. V A). System 2, state point 1.

V. RESULTS FOR THE ISOTOPIC MIXTURES

A. The Green-Kubo integrand for D^T of system 2

According to Eqs. (1a)–(3) given in Sec. II, the total Green-Kubo integrand $\langle \mathbf{J}_m(0)\mathbf{J}_q(t)\rangle$, is composed of three terms, $\langle \mathbf{J}_m(0)\mathbf{J}_q^{\rm kin}(t)\rangle$, $\langle \mathbf{J}_m(0)\mathbf{J}_q^{\rm pot}(t)\rangle$, and $\langle \mathbf{J}_m(0)J_q^{\rm ent}(t)\rangle$, where $\mathbf{J}_q^{\rm kin}$ denotes the first part of the right-hand side of Eq. (2a), $\mathbf{J}_q^{\rm pot}$ the second one and $\mathbf{J}_q^{\rm ent}$ the third one containing the partial enthalpies. We shall call these partial Green-Kubo integrands kinetic-diffusive (KD), potential-diffusive (PD), and enthalpic-diffusive (ED) terms. Their sum gives the total cross-correlation function.

For system 2 (mass ratio: $m_2/m_1=2$), we have computed these four CCF's, and the results are plotted in Figs. 2 and 3. As the total CCF starts from zero, we show the function in units of 10^{10} cm^2/s^2 normalized such that its integral over real time gives $(3/\rho)D^T$. Evidently, all the functions have amplitudes of the same order of magnitude. So the three partial CCF's determine the total one by about the same weight. Furthermore, the short-time behavior of the total CCF is governed by a cancellation of the PD term on one hand and the KD and ED terms on the other hand.

So it is crucial to compute reliably the ED function which contains the partial enthalpies. This is completely different from the situation for the autocorrelation function of the thermal conductivity where the terms involving h_α do not contribute significantly.[20] Comparing the plots in Figs. 2 and 3, we find the following.

(i) The short-time behavior of the total CCF is governed by all the three partial CCF, while the behavior at longer times is represented by the PD term alone.

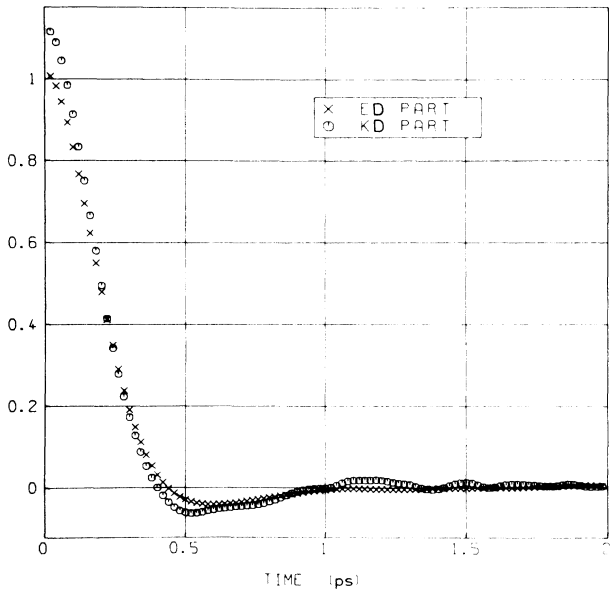

FIG. 3. Partial CCF's, kinetic-diffusive term, and enthalpic-diffusive term, of System 2 at state point 1.

(ii) The partial terms, KD and ED, have a smooth form and decay quickly; the PD term displays fluctuations and dies away after about 1.2 ps.

(iii) KD and ED terms show an inverse time behavior in comparison with the PD term, but this is peculiar to the isotopic mixture.

(iv) The total CCF has a characteristic form found for all the mixture systems considered, namely, a pro-

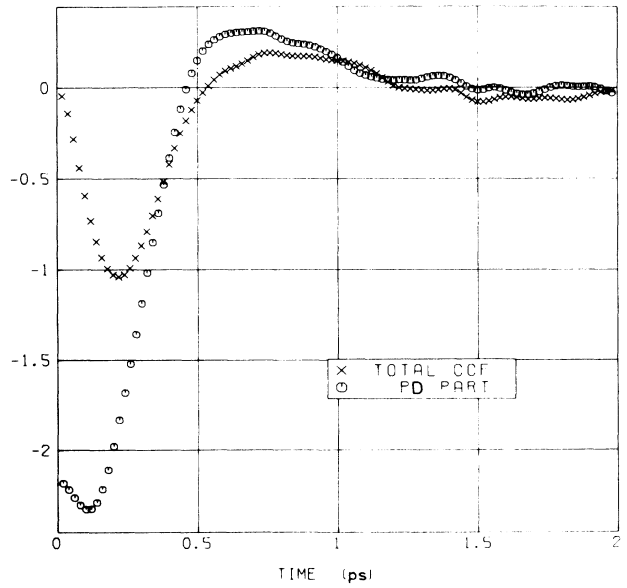

FIG. 2. Total Green-Kubo integrand for D^T (CCF) and the partial, potential-diffusive CCF of system 2 at state point 1. The partial function has the same units as the total one.

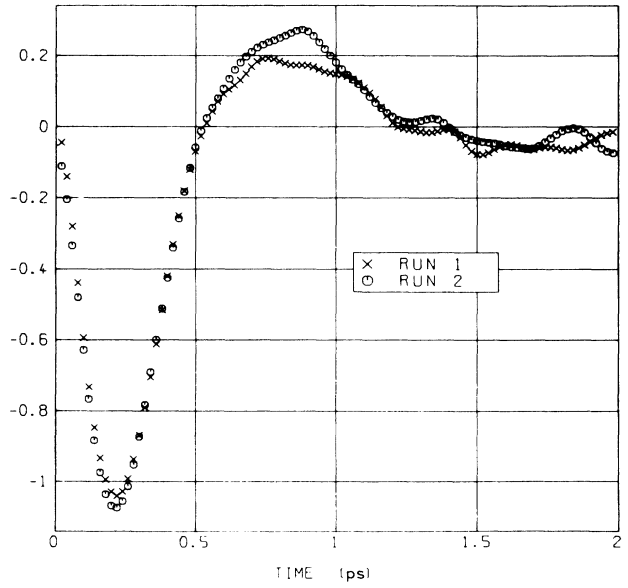

FIG. 4. Total CCF calculated from two different runs (see Table IV). System 2, state point 1.

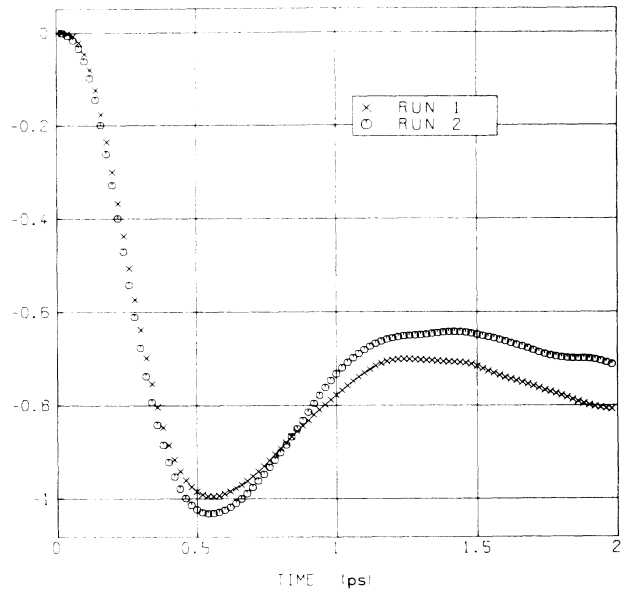

FIG. 5. Time integrals obtained from the CCF's shown in Fig. 4.

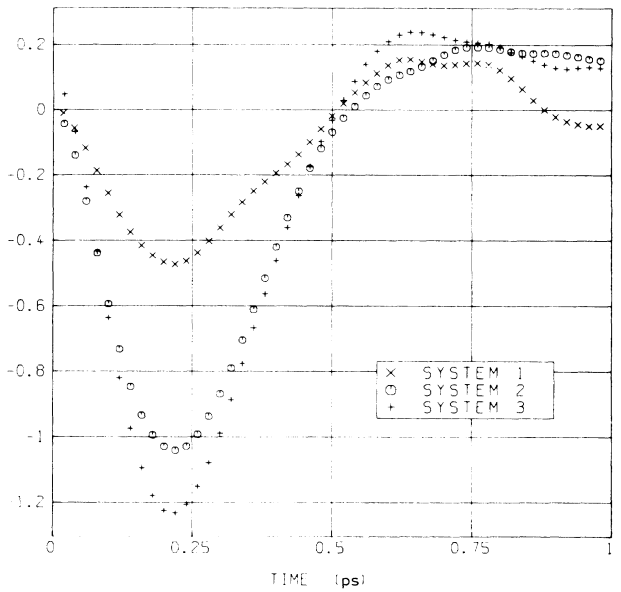

FIG. 6. Total CCF's of systems 1–3.

nounced negative part at short times and a longer ranged positive part.

The thermal diffusion coefficient is given by the time integral over the total CCF. From point (iv) it becomes immediately clear that the integral value must be approximately 0 due to the cancellation of the negative and the positive areas enclosed by the correlation function. While the first negative part of the CCF can be obtained with relatively high accuracy, the second positive one cannot, because of statistical fluctuations noticeable in that branch of the curve. For illustration, we have plotted CCF's of two different runs in Fig. 4 and the time integrals in Fig. 5. We see that the plateau values are not very pronounced and differ appreciably in height.

Our further computations have, however, indicated that the integration should be performed up to the time where the second positive branch of the total CCF or the PD term gets close to zero. The behavior of the CCF for longer times seems to be mainly governed by statistical fluctuations. By seven independent computations we have evaluated the thermal diffusion coefficient for system 2. These coefficients, the mutual diffusion coefficients, and the thermal conductivities are given in Table IV. The average values and our estimated errors are additionally listed in the table. As expected, the accuracy of this cross coefficients amounts to about 20%.

B. D^T values for systems 1 and 3

For the mass ratios, $m_2/m_1=1.4$ and 2.5, we have performed only two runs for each system. To illustrate the alteration of the CCF's we display plots of these functions for systems 1–3 in Fig. 6.

As expected, only the amplitudes of the correlation functions vary giving a D^T value growing monotonously from system 1 to system 3. The values are summarized in Table V together with the other transport coefficients and the estimated error bars.

The increase of the thermal diffusion constant (absolute value) with the mass ratio seems to be reasonable. Indeed it is known experimentally from investigations on binary gas mixtures[2,21,22] that the separation tendency of the components increases with the mass ratio.

TABLE IV. Transport coefficients of system 2 calculated by MD for state point 1. N represents particle number; Δt, total integration time; ρ, mass density.

Run	N	Δt (ns)	$10^5\frac{1}{\rho}D^T$ (cm^2s^{-1})	10^3 s (K^{-1})	$10^5 D_{12}$ (cm^2s^{-1})	$10^3\lambda$ ($JK^{-1}m^{-1}s^{-1}$)	Comments
1	108	16.0	−0.57±0.15		3.92±0.2	71.6±2	Error bars for runs 1–4
2	108	16.0	−0.78		3.76	71.9	
3	108	16.0	−0.66		3.78	70.4	
4	108	16.0	−0.63		3.99	71.2	
5	256	7.0	−0.52±0.2		3.98±0.25	68.0±3	Error bars for runs 5–7
6	256	9.0	−0.86		4.02	73.1	
7	256	8.2	−0.56		3.77	71.8	
			−0.65±0.1	+ 5.5±1.5	3.89±0.1	71.1±1	Mean values

TABLE V. Transport coefficients of systems 1–3 computed by MD for state point 1.

System	N	Δt (ns)	$10^5 \frac{1}{\rho} D^T$ ($cm^2 s^{-1}$)	10^3 s (K^{-1})	$10^5 D_{12}$ ($cm^2 s^{-1}$)	$10^3 \lambda$ ($JK^{-1}m^{-1}s^{-1}$)	Comments
1	108	16	−0.20±0.2		3.72±0.2	76.9±2.0	
1	108	16	−0.40		3.73	77.2	
1			−0.30±0.2	+2.4±1.7	3.73±0.15	77.1±1.5	Mean values
2			−0.65±0.1	+5.5±1.0	3.89±0.1	71.1±1.0	Mean values (from Table IV)
3	108	16	−0.73±0.15		3.79±0.2	66.3±2.0	
3	108	16	−0.75		3.67	66.3	
3			−0.74±0.15	+7.1±1.8	3.73±0.15	66.3±1.5	Mean values

Furthermore, the negative sign of D^T is also in agreement with experimental results for binary liquid mixtures. According to our definitions (see Ref. 1) a *positive* D^T indicates that the considered species (here component 1) diffuses *down* the temperature gradient, a negative D^T denotes diffusion upwards the temperature gradient. In experiments with two-component liquid systems a negative D^T is always measured when the mass ratio is large and the first component has the lighter mass.[23] In other words, for liquid mixtures with thermal diffusion governed by the mass ratio the species of the lighter mass migrates always upwards the temperature gradient. This is precisely what we have found for our isotopic model mixtures.

VI. RESULTS FOR THE Ar-Kr MODEL MIXTURES

A. Green-Kubo integrand for D^T

As in Sec. V, we show the total Green-Kubo integrand and the partial ones of the Ar-Kr system in Figs. 7 and 8. Although the total CCF for Ar-Kr resembles that of system 2, the ED term is initially *negative* and larger in amplitude than the KD or the PD term. Such a change of the ED part of the CCF is of course a consequence of the differences between the three interatomic potentials assumed for this mixture.

In Figs. 9 and 10 obtained via two different runs, we compare the total CCF's and the time integrals. Similarly to the case of system 2 we find that the area corresponding to the first part of the CCF nearly compensates that of the second part so that the asymptotic value of the time integral is quite small.

The statistical fluctuations in the CCF for longer times make it difficult to detect a plateau value as is seen by the first plot in Figs. 9 and 10. However, to demonstrate convincingly that the CCF is essentially determined by noise for times larger than about 1.2 ps, we have averaged the CCF over six independent runs. The result is shown in Fig. 11. For comparison the CCF of system 2 averaged in the same way is presented in Fig. 12. Both CCF's exhibit now the expected behavior: a

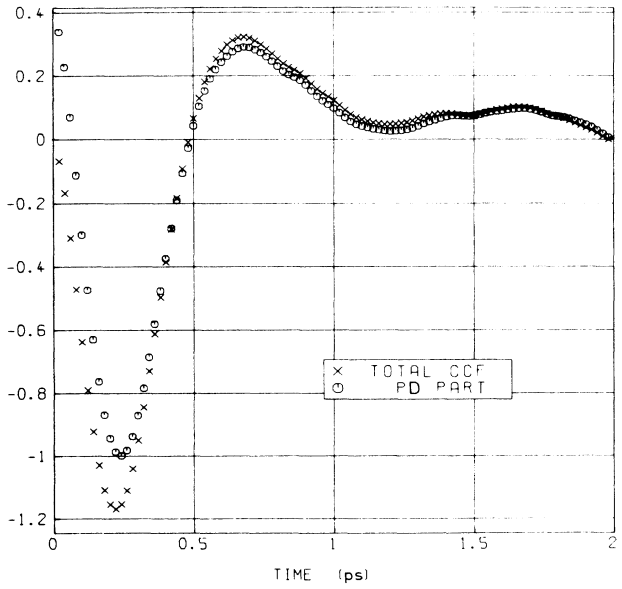

FIG. 7. As in Fig. 2, but for the LJ Ar-Kr system at state point 2.

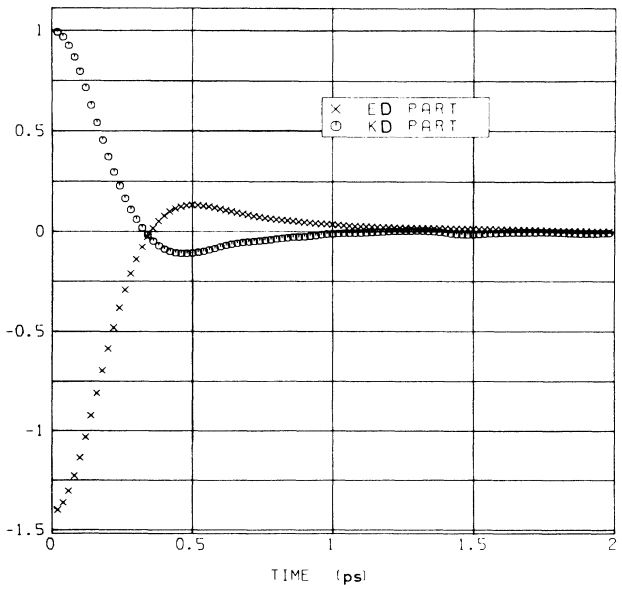

FIG. 8. As in Fig. 3, but for the LJ Ar-Kr system at state point 2.

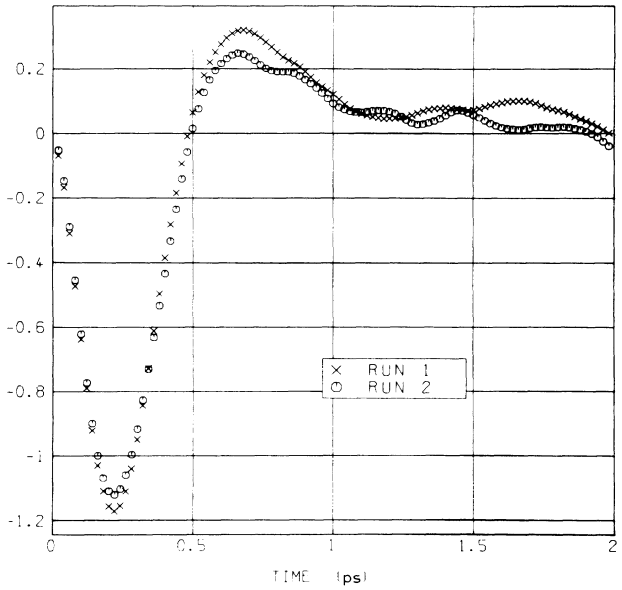

FIG. 9. As in Fig. 4, but for Ar-Kr at state point 2.

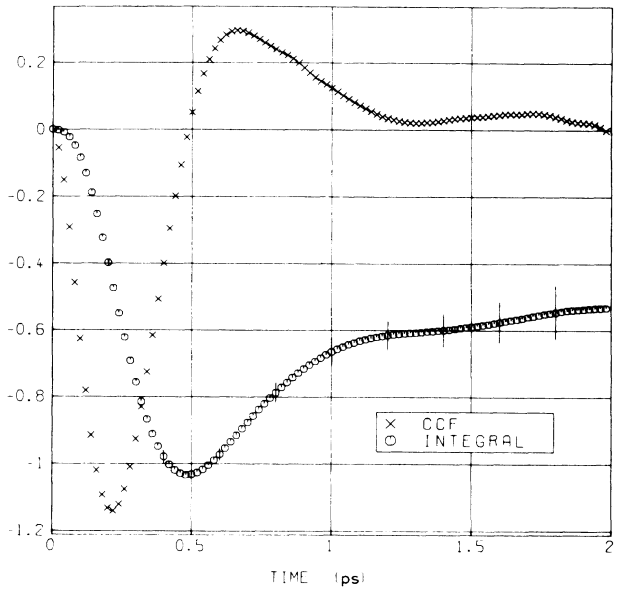

FIG. 11. Comparison of the total CCF and its time integral. Ar-Kr system at state 2. The CCF is averaged over six curves obtained by single MD runs. Vertical lines indicate error bars.

pronounced first negative part, a second longer ranged positive part vanishing approximately for times larger than about 1.2 ps. Accordingly the integrals, also given in Figs. 11 and 12, show rather good plateau regions and lead to fairly accurate cross coefficients.

We have listed the thermal diffusion coefficient, the mutual diffusion coefficient and the thermal conductivity obtained by these independent runs in Table VI together with their mean values and the estimated statistical error.

The indicated error bars for D^T take into account only the statistical uncertainty of the computations, not the systematic errors due to the molecular approximation which we have used for the partial enthalpies (see discussion). However, as the Ar-Kr system is not a very nonideal mixture,[15] we believe that these systematic errors are negligible in comparison with the statistical error of about 20%.

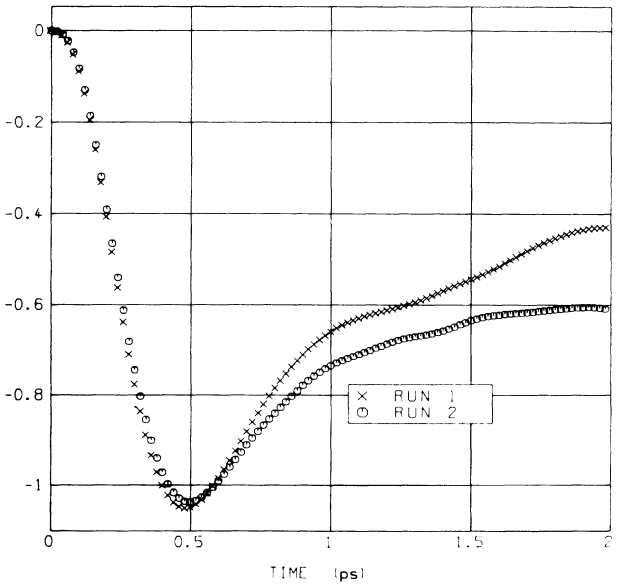

FIG. 10. Time integrals obtained from the CCF's shown in Fig. 9.

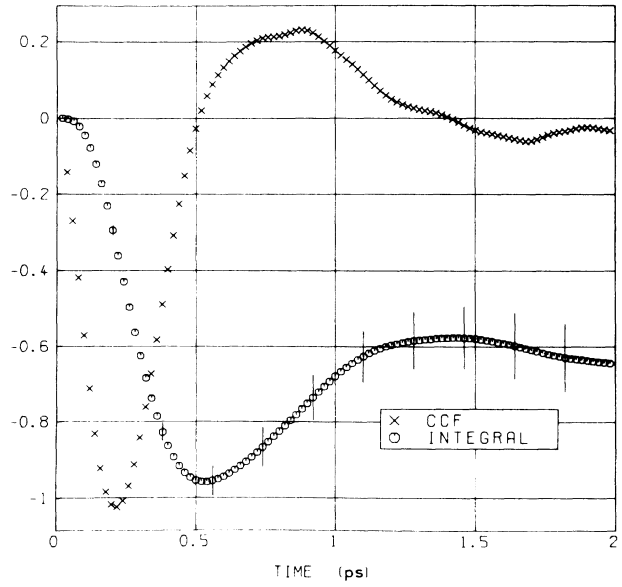

FIG. 12. As in Fig. 11, but for system 2. The CCF is averaged over seven independent curves.

TABLE VI. Transport coefficients of LJ Ar-Kr at state points 2–3.

Run	State point	N	Δt (ns)	$10^5 \frac{1}{\rho} D^T$ ($cm^2 s^{-1}$)	10^3 s (K^{-1})	$10^5 D_{12}$ ($cm^2 s^{-1}$)	$10^3 \lambda$ ($JK^{-1}m^{-1}s^{-1}$)	Comments
1	2	108	16	−0.45±0.2		2.39±0.15	83.0±2.0	
2	2	108	16	−0.64		2.38	82.4	
3	2	108	16	−0.65		2.39	84.1	
4	2	108	16	−0.37		2.39	81.6	
5	2	108	16	−0.59		2.44	82.3	
6	2	256	4	−0.65		2.47	84.3	
	2			−0.56±0.1	+9.1±2.0	2.41±0.1	83.0±1.0	Mean values
1	3	108	8	−0.44±0.2		2.63±0.15	77.3±2.0	
2	3	108	8	−0.48		2.67	80.5	
3	3	108	8	−0.38		2.58	80.0	
4	3	108	16	−0.43		2.65	79.4	
				−0.43±0.13	+6.5±2.0	2.65±0.12	79.3±1.3	Mean values

B. Comparison with NEMD results

For state point 2 of the Ar-Kr model system two existing nonequilibrium MD studies can be used for direct comparisons. MacGowan and Evans[5] (ME) have used a well-established NEMD method and runs of total integration times comparable to ours. These authors define the heat current in the mixture in terms of instantaneous variables thereby using the molecular approximation for the partial enthalpies, as already mentioned (see Sec. V). Paolini and Ciccotti[6] (PC) have used the same NEMD method as ME, however, a substraction technique[24] was additionally exploited to avoid largely the problem of extrapolation to zero field necessary for NEMD calculations[25] when transport coefficients are to be evaluated. However, the total integration time of the computations of PC was shorter than that performed by ME and our work.

The comparison of the transport coefficients is made in Table VII, where some additional details on the NEMD and MD runs are also given. We see that excellent agreement exists for the NEMD values of ME and the results of the present work. The difference lies well within the error bars. Interesting is the following point: in their work ME claim to have discovered a significant difference in the mutual diffusion coefficients determined by their NEMD and previous MD by Schoen and Hoheisel.[8] There is, however, a simple explanation for this discrepancy. The D_{12} values in Ref. 8 were obtained with large particle numbers of 864 and more, while the values found by ME and in the present work stem from computations with 108–256 particles. For these small particle numbers—not studied in Ref. 8–a tendency towards lower diffusion coefficients can easily be shown.

In Table VIII we show some results for the mutual diffusion coefficient with different particle numbers and runs of a total integration time of 1000 ps. Taking into account this particle number dependence, the D_{12} values determined in Refs. 5 and 8 and the present work are in good agreement. The cross ratio $D_{12}/(x_1 D_2 + x_2 D_1)$ with D_1 and D_2 being the self-diffusion coefficients, defined in Ref. 8 appears to be almost independent of the particle number. This ratio is also shown in Table VIII. Even for a 32-particle system, there is no significant difference between our results and those of Ref. 8, though a slight tendency towards smaller values for smaller MD systems can be read from Fig. 6 of that work.

TABLE VII. Comparison of NEMD and MD values for the transport coefficients of LJ Ar-Kr.

Method	N	Δt (ns)	n^*	T^*	$10^5 \frac{1}{\rho} D^T$ ($cm^2 s^{-1}$)	10^3 s (K^{-1})	$10^5 D_{12}$ ($cm^2 s^{-1}$)	$10^3 \lambda$ ($Jm^{-1}K^{-1}s^{-1}$)
NEMD Ref. 5	108 and 256	8	0.7902	0.805	−0.68±0.2	11.3	2.38±0.17	79.4±1.2
MD This work	108	16	0.7902	0.803	−0.43±0.13	6.5	2.64±0.12	79.3±1.3
	32[a]	4			−0.45±0.2			
	32[b]	4			−0.48±0.2			
NEMD This work	32	4	0.7902	0.803	−0.34±0.2			
NEMD Ref. 6	256	0.8	0.7902	0.824	−1.2±0.2	16.2	2.86±0.07	84.1±1.7

[a]Calculated with the Bochum program.
[b]Calculated with the Rome program.

TABLE VIII. Mutual diffusion coefficient of LJ Ar-Kr determined by MD as a function of the particle number. State point, $n^*=0.7889$; $T^*=0.812$; $x_1=0.5$.

N	$10^5 D_{12}$ ($cm^2 s^{-1}$)	$\frac{D_{12}}{x_1 D_2 + x_2 D_1}$ [a]	Comment
32	2.24	1.02	
108	2.35	0.88	
256	2.57	0.91	
500	2.79	1.02	
	2.86	1.05	From Ref. 8

[a] D_1, D_2 self-diffusion coefficients.

On comparing our transport coefficients with the NEMD results of PC in Ref. 6, we find disagreement within the error bars. However, as the temperature of the state chosen by PC, is 2.5% higher than ours, the mutual diffusion coefficient and the thermal conductivity may be regarded as consistent with our values. The discrepancies in D_{12} and λ are only small and the PC values exceed our MD results most likely due to the higher temperature.

In contrast, the thermal diffusion coefficient (absolute amount) determined by PC exceeds the value of this work by about a factor of 2. Comparison with the CCF which was also computed by PC showed that the first minimum of the curve is much deeper than the one found in this work. The maxima of both functions are however nearly equal. As the Green-Kubo results complementarily obtained by PC showed a similar tendency, we attempted to study these discrepancies by further computations. We performed runs of total time length of 4000 ps with a 32-particle system using the "Rome program" and the "Bochum program." The resulting CCF's are plotted in Fig. 13, and the thermal diffusion coefficients are given in Table VII. While the transport coefficients determined with both programmes are now in best agreement, the CCF's differ clearly in amplitude.

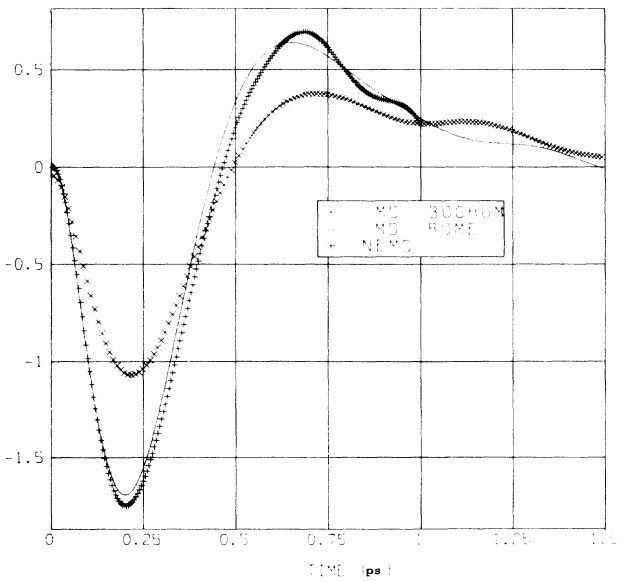

FIG. 13. CCF's for Ar-Kr at state point 3. $\times$ denotes MD with the Bochum-program (this work); ——, MD with the Rome-program (this work); +, NEMD (this work). All the calculations were done with a 32-particle system.

Compared with the results obtained by the "Bochum program," the "Rome program" gives more pronounced maxima and minima of the CCF. Integration of the curves leads of course to the some results for the transport coefficient due to the cancellation of positive and negative areas. At present, we have no satisfactory explanation for this remaining discrepancy. Further calculations with a soft sphere potential are, however, in preparation.

Nevertheless, the thermal diffusion coefficients determined by these latter calculations are in good agreement and agree moreover with the best value obtained with larger particle numbers (see Table VII). This indicates a very small particle number dependence of D^T, similar to the cross-ratio discussed before.

The relatively large D^T value found by PC might probably be the consequence of too short MD runs which cannot reproduce the maximum of the CCF at longer times. Our studies have shown that computations of a total integration time of at least 3 ns are necessary to predict reliable values for the cross coefficient. A nice illustration of this is given by plots of the total CCF evaluated at very different averaging levels in Fig. 14. In fact the CCF's have been obtained by data from one single run of 16 ns (total integration time). For the first CCF, we considered only the first part of the data up to 1 ns, for the second curve only the part of the data up to 2 ns and so on. The averaging process included at least 50.000 events corresponding to about 5.000 uncorrelated time origins. The plots in Fig. 14 clearly show how the time behavior of the CCF is altered when increasing the integration time. For total integration times longer than 3 ns, a definite form of the CCF is reached, supporting our previous statements. The cross transport coefficient resulting from these CCF's plotted in Fig. 14 are summarized in Table IX. We see rather well the evolution of the D^T value finally being consistent with the result given in Table IV.

C. Comparison with experiment

A direct comparison of our calculated Soret coefficients with experiment cannot be made, as unfor-

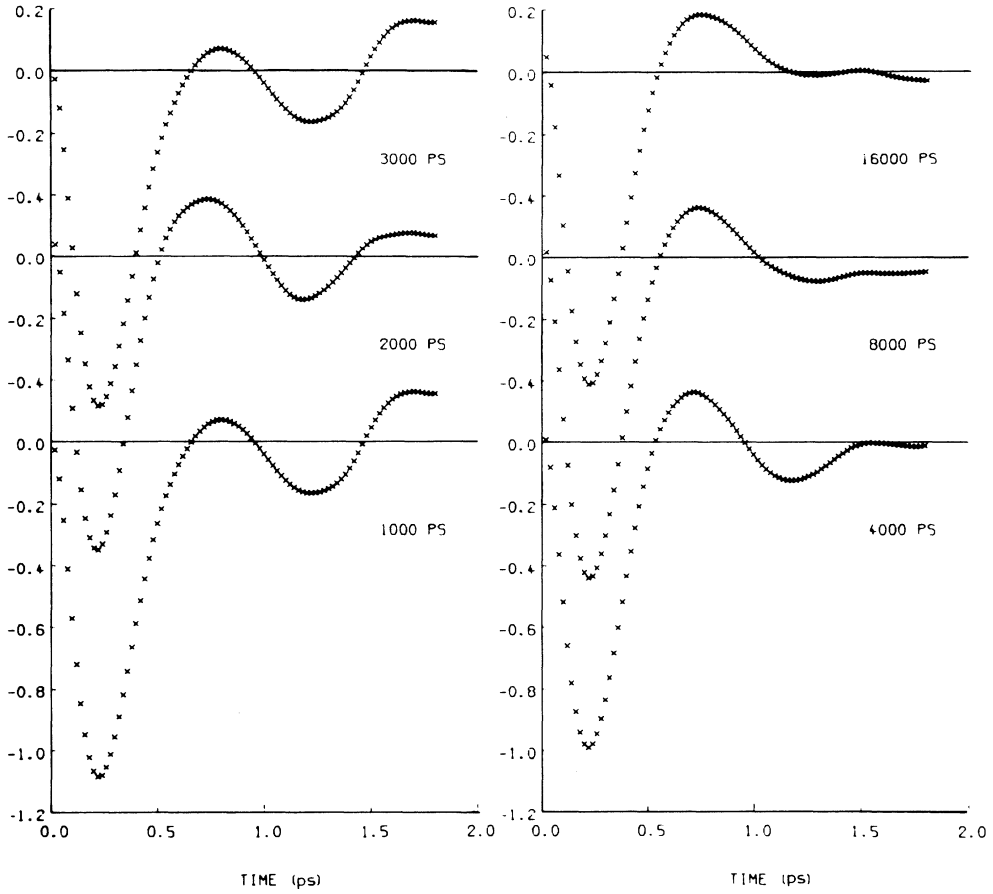

FIG. 14. CCF's of system 2 using increasingly larger parts of the trajectories for the averaging process (see Table IX). The actual integration time is indicated in the figure.

tunately no measurements are available for rare-gas liquid mixtures. However, Soret coefficients for several mixtures of organic liquids have been experimentally measured so far.[23] As all these values range at the order of magnitude of 10^{-3} K^{-1}, we expect the same order of magnitude for liquid rare-gas mixtures. In fact our numerical results for s of LJ Ar-Kr mixtures fall well in line with this experimental range. For liquid mixtures with very large mass ratios, we expect s to be essentially determined by this mass effect when the mixture is not too nonideal (hydrogen bonding, association, etc.) We have gathered some experimental values of s for mixtures with mass ratios of the same order of those of the Ar-Kr system and system 2 in Table X. The table shows that the predicted Soret coefficients, for model Ar-Kr and the isotopic system 2, agree in the order of magnitude with the experimental data.

TABLE IX. Thermal diffusion coefficient obtained from the cross correlation curves plotted in Fig. 14.

Δt (ns)	$10^5 \frac{1}{\rho} D^T$ ($cm^2 s^{-1}$)	Comments
1.0	−1.10	run 2 for system 2
2.0	−0.72	was used; the CCF's
3.0	−0.74	were integrated up
4.0	−0.79	until ~1 ps
8.0	−0.85	
16.0	−0.78	
	−0.65	Best value (see Table IV)

VII. DISCUSSION AND CONCLUSIONS

We have shown that the Soret coefficient of the Lennard-Jones mixture can be reliably computed via equilibrium MD. Using MD runs of a factor of 10 longer than those commonly carried out for transport coefficients, we were able to determine the Soret coefficient with an accuracy of better than 30%. Agreement with NEMD results is remarkable, demonstrating that both methods can equivalently by employed to determine transport coefficients of simple liquid mixtures.

While for the isotopic mixtures, our calculations do not involve any systematic error due to insufficient determination of the partial enthalpies, for the Ar-Kr mixture the molecular approximation for h_α is not exact. The h_α's can be determined by computing the total enthalpy

TABLE X. Soret coefficient for some experimental (Ref. 23) equimolar mixtures compared with theoretical values of this work.

Liquid mixture	Mass ratio m_1/m_2	10^3 s (K^{-1})
C_6H_6-CCl_4	0.51	+4.6
C_6H_{12}-CCl_4	0.55	+4.7
CCl_4-CBr_4	0.46	+5.0
Ar-Kr (this work)	0.48	+9.1[a]
Isotopic system 2 (this work)	0.50	+5.5

[a]State point 2.

as a function of composition. The partial enthalpies are then obtained by constructing the tangents of the resulting curve.[15]

Fortunately McDonald[26,27] calculated the total enthalpy h of LJ Ar-Kr as function of concentration. From these calculations a linear behavior of h results, giving directly the partial enthalpies. Apparently the LJ Ar-Kr mixture behaves very ideally and has a low excess enthalpy. Though the computations of McDonald[26] have been made at constant pressure, for constant volume mixing a similar ideal behavior is expected. Furthermore, the state chosen in Ref. 26 does not correspond precisely to the state considered herein. Nevertheless, the results given in Ref. 26 should to a good approximation hold for our state. Using these h values, we find partial enthalpies of

$$-h_1 = 5.19\epsilon_{11}/Nk_BT ,$$

$$-h_2 = 8.98\epsilon_{11}/Nk_BT ,$$

(without kinetic contributions) which agree well with the results obtained by our molecular approximation:

$$-h_1^{\text{appr}} = 5.40\epsilon_{11}/Nk_BT ,$$

$$-h_2^{\text{appr}} = 8.19\epsilon_{11}/Nk_BT .$$

This shows that at least for these simple binary mixtures the molecular approximation for h_α works well, as expected. For very nonideal systems, as the ones studied, for example, by Gillan,[16] the discrepancy between h_α and h_α^{appr} might become significant, and then an appropriate evaluation of h_α by separate MD methods is inevitable.

We purposely passed over a comparison of the Dufour and the Soret effect, though we have studied both extensively. As these investigations revealed many interesting results, we shall present them in a separate paper.

In fact, all the cross correlation functions shown in this work are averages over Soret and Dufour–type functions. The Dufour-type CF is defined by Eq. (3), while the Soret-type CF may be obtained by interchanging the time dependence in Eq. (3). In a later paper, we shall report our studies on the potential parameter dependence of the Soret coefficient.

ACKNOWLEDGMENTS

We thank D. J. Evans, M. Gillan, and W. G. Hoover for interesting discussions during a Centre Européen de Calcul Atomique et Moléculaire (CECAM) workshop organized by one of us (G.C.) and W. G. Hoover, and we are grateful to the director of CECAM, C. Moser, for his kind hospitality. Furthermore, we thank B. Klare and U. Krupinski for help. Sufficient computation time was granted by the Rechenzentrum der Ruhr-Universität Bochum (Control Data Corporation Cyber 205 computer), and financial support was given by the Deutsche Forschungsgemeinschaft (Ho 626/6-2).

[1]D. D. Fitts, *Nonequilibrium Thermodynamics* (McGraw-Hill, New York, 1962).
[2]K. E. Grew, in *Transport Phenomena in Fluids,* edited by H. J. M. Hanley (Marcel Dekker, London, 1969).
[3]H. J. M. Hanley, in *Transport Phenomena in Fluids,* Ref. 2.
[4]B. J. Berne and R. Pecora, *Dynamic Light Scattering* (Wiley, New York, 1976).
[5]D. MacGowan and D. J. Evans, Phys. Rev. A **34**, 2133 (1986).
[6]G. V. Paolini and G. Ciccotti, Phys. Rev. A **35**, 5156 (1987).
[7]D. L. Jolly and R. J. Bearman, Mol. Phys. **41**, 137 (1980).
[8]M. Schoen and C. Hoheisel, Mol. Phys. **52**, 33 (1984).
[9]M. Schoen and C. Hoheisel, Mol. Phys. **52**, 1029 (1984).
[10]K. E. Gubbins, in *Statistical Mechanics,* edited by K. Singer (The Chemical Society, London, 1973), Vol. 1.
[11]W. A. Steele, in *Transport Phenomena in Fluids,* Ref. 2.
[12]J. H. Irving and J. G. Kirkwood, J. Chem. Phys. **18**, 817 (1950).
[13]R. J. Bearman and J. G. Kirkwood, J. Chem. Phys. **28**, 136 (1958).
[14]R. J. Bearman, J. Chem. Phys. **29**, 1278 (1958).
[15]J. S. Rowlinson and F. L. Swinton, *Liquids and Liquid Mixtures* (Butterworths, London, 1982).
[16]M. J. Gillan, J. Phys. C (to be published).
[17]C. Hoheisel and U. Deiters, Mol. Phys. **37**, 95 (1979).
[18]R. Vogelsang and C. Hoheisel, Phys. Rev. A **35**, 3487 (1987).
[19]R. Vogelsang, C. Hoheisel, and G. Ciccotti, J. Chem. Phys. **86**, 6371 (1987).
[20]C. Hoheisel and M. D. Zeidler, Mol. Phys. **54**, 1275 (1985).
[21]K. E. Grew and T. L. Ibbs, *Thermal Diffusion in Gases* (Cambridge University Press, Cambridge, England, 1952).
[22]H. Röck and W. Köhler, *Ausgewählte moderne Trennverfahren mit Anwendungen auf organische Stoffe,* edited by W. Jost (D. Steinkopff-Verlag, Darmstadt, 1965).
[23]Landolt-Börnstein, Zahlenwerte und Funktionen, Bd. Transport *Phänomene II* (Springer, Berlin, 1968).
[24]G. Ciccotti, G. Jacucci, and I. R. McDonald, J. Stat. Phys. **21**, 1 (1979).
[25]W. G. Hoover, Ann. Rev. Phys. Chem. **34**, 103 (1983).
[26]I. R. McDonald, Mol. Phys. **23**, 41 (1972).
[27]I. R. McDonald, in *Statistical Mechanics,* Ref. 10.